NURETH14-421

COUPLED NUCLEAR-THERMAL-HYDRAULIC CALCULATIONS FOR FORT ST. VRAIN REACTOR

Benjamin R. Betzler, Eva E. Sunny, John C. Lee, William R. Martin Department of Nuclear Engineering and Radiological Sciences University of Michigan, Ann Arbor

Abstract

The 842-MWt Fort St. Vrain (FSV) helium-cooled, graphite-moderated reactor was officially decommissioned in 1989 after 14 years of operation. The active core has 247 fuel columns divided into 37 fuel regions, with six axial layers of 79 cm tall hexagonal fuel blocks. Graphite blocks outside, above, and below the active core serve as reflectors. Four types of blended TRISO particles produce the 13 compositions distributed in the fuel regions. An MNCP5 model for FSV uses an average kernel size that preserves fuel loading and a 58% packing fraction for each composition, either smearing TRISO particles within the fuel rod or explicitly modeling each particle in a regular lattice. A coupled MCNP5-RELAP5 setup accounts for thermal feedback effects. For eight axial and six radial regions of the FSV model, MCNP5 determines the power fractions required by RELAP5 to calculate axial temperature distributions. The MCNP5 model receives these temperatures and the process repeats until convergence to a solution. Similar work on the Very High Temperature Reactor uses Ratio and PIKMT methods for both homogeneous and heterogeneous models. Both methods calculate energy deposition from neutrons, fission products, beta particles, and prompt and capture gammas, but the Ratio method uses pre-calculated fractions to account for delayed gamma contributions to energy deposited. The PIKMT method is computationally costlier, more accurate, and converges faster than the Ratio method. The PIKMT method is applied to FSV.

Introduction

The Fort St. Vrain (FSV) reactor is a 842-MWt, helium-cooled, General Atomics (GA) High Temperature Reactor (HTR), which first achieved criticality in 1975. The active core has 37 fuel regions, which produce power from a 93% high enriched uranium (HEU) and thorium based fuel cycle [1]. The purpose of this project is to model the initial configuration for FSV based on neutronic and thermal-hydraulic data available. A 3-D MCNP5 [2] model provides neutronic analysis and a 1-D RELAP5 [3] thermal-hydraulic model provides temperature data. Python [4] scripts transfer power fractions and temperature distributions between the two models, creating a loosely coupled setup. The process repeats until reaching a solution. The iterative process is known as the PIKMT method [5]. The Root-Mean-Squared Deviation (RMSD) between consecutive iterations measures convergence.

The active core contains hexagonal fuel assemblies with a height of 79.3 cm and a flat-to-flat distance of 36.0 cm. Cylindrical fuel compacts with a radius of 0.625 cm and a height of 5.0 cm fill the fuel holes in the assemblies. Four types of fuel kernels pack the fuel compacts: two sizes of fertile and two sizes of fissile particles. Small and large diameter ranges differentiate size. The initial asymmetric fuel loading requires particles mixed in specific ratios to achieve the 13 unique fuel blends. The active core has 247 fuel columns of six axially-stacked fuel blocks. Sixty-six hexagonal replaceable reflectors sit radially adjacent to the active core and 24 irregularly-shaped permanent reflectors sit outside the replaceable reflectors [1]. Regulatory constraints limited the initial critical configuration to a fraction of full power [6] and the RELAP5 model reflects the decreased flow and pressure.

Drawing from HTR operating experience is important to VHTR research. We have FSV data to benchmark the MCNP5-RELAP5 setup. Thus, when we use this method for analyzing NGNP VHTRs, we know with a degree of certainty that it accurately predicts trends or behaviors. MCNP5 provides very accurate neutronic analysis, and Idaho National Lab uses RELAP5 for VHTR thermal hydraulics.

1. MCNP5 Model

The MCNP5 model is built to known FSV technical specifications. Fuel block models account for handling holes, dowel pins, and burnable poison loadings. The model conserves the number of fuel compacts in each block [7]. For this coupled application, a single homogenized material represents the fuel compacts; the model smears individual TRISO particles with the surrounding graphite. A fully heterogeneous MCNP5 model runs in 3 to 7 days, too lengthy for this coupled setup. Results from homogeneous and heterogeneous models of the Very High Temperature Reactor (VHTR) simulations indicate that the effect of modeling the particle fuel is noticeable but not significant with respect to the converged power distribution [5].

The FSV MCNP5 model has eight axial temperature zones: six for each block of the active core and two for the top and bottom reflectors. Radially, the model has six temperature zones: four fuel regions, a replaceable reflector region, and a permanent reflector region. Figure 1 shows these radial zones. The 48 individual temperature zones in the model stretches this version of MCNP5 to its limits, making finer resolution is difficult. The asymmetric fuel loading and temperatures push the model to the MCNP5 universe limit.

The FSV MCNP5 input decks are typically 25,000 lines. A Python script rewrites the input deck to reflect desired changes such as tally types, boron impurities, and fuel loading [7]. It also adjusts material temperatures crucial for coupling to RELAP5.

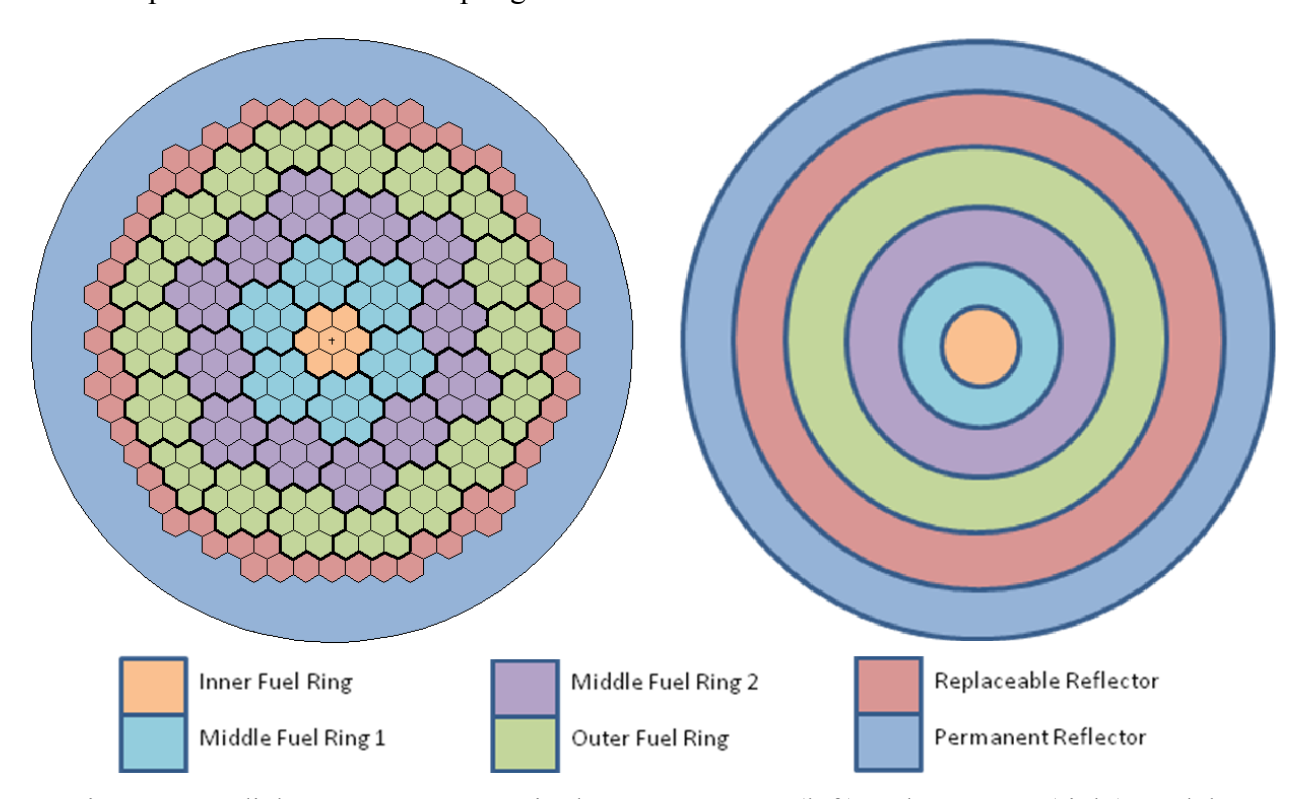


Figure 1 Radial temperature zones in the FSV MCNP5 (left) and RELAP5 (right) models.

Each MCNP5 run has 500 inactive cycles for source convergence, and 600 active cycles. Each cycle has 250,000 histories. Runs result in a final k-effective standard deviation of 6 pcm. Location and material compositions determine standard deviations of heat deposition tallies. A *standard* and *pikmt* run determine the heat deposition within the MCNP5 FSV model. The *standard* and *pikmt* runs take 18 and 28 hours, respectively, on 32 2.2 GHz cores.

The pseudo-material construct [8] interpolates between ENDF/B-VI.8 cross sections at temperature intervals of 100K to obtain cross sections at specific temperatures. The $S(\alpha,\beta)$ tables for graphite are from ENDF/B-VI.3 at 294K [2]. A stochastic verification [7] of the MCNP5 model fuel loading shows that it is well within 0.1% of the as-built loading [9].

2. RELAP5 Model

The RELAP5 1-D model has six radial rings with eight axial planes to reflect the FSV MCNP5 model. Figure 1 shows a radial layout of the model. The four fuel rings have six axial fuel regions between top and bottom reflectors to form eight axial planes, while replaceable and permanent reflector rings have eight axial planes of graphite. Figure 2 shows these axial divisions.

Due to licensing constraints, the initial configuration of FSV only reached a fraction of full power before reloading. The RELAP5 model reflects the initial configuration at this reduced thermal power, with the inlet pressure, core pressure drop, and total mass flow through the circulator adjusted accordingly [6].

The two types of fuel blocks in the active core are standard and control blocks. Both types have a fuel handling hole, but standard blocks have 108 coolant channels and control blocks have 57 coolant channels, 2 control rod channels, and 1 reserve shutdown hole. The center block of each fuel region is a control block. Figure 2 shows the numbers of each block type in the radial rings. Gaps between blocks are 2 mm [1]. The permanent reflector region has 1 mm gaps between irregular reflectors.

The total flow area in RELAP5 accounts for all coolant paths including gaps between blocks. Because the RELAP5 model is 1-D, the total number of coolant channels must represent the height of each fuel region. Thus, the RELAP5 area factor adjusts the heat transfer length, multiplying the number of coolant channels in each region by the axial plane height in Figure 2. Equation 1 calculates the area factor, 22, where 22 is the number of coolant channels in a block, 22 is the number of blocks, and 2 is the axial region height. Figure 2 lists area factors in parenthesis for each core zone.

$$?? = ?? \times ?? \times ?$$
 (1)

$$22 = 3.38 + 2.74 \times 10 - 22 - 4.88 \times 10 - 622 - 0.146 \times 1062 - 2/222/2$$
 232] (2)

Table 1 Thermal conductivity for bonded fuel compact with 11.5% fissile and 50.5% fertile particles.

Temperature [K]	Thermal Conductivity [W/m-K]
672.2	12.14
811.1	10.89
950	9.93
1088.9	9.15
1227.8	8.49
1366.7	7.92

Table 2 Volumetric heat capacity for the bonded fuel compact with 11.5% fissile and 50.5% fertile particles.

Temperature [K]	Volumetric Heat Capacity [J/m³-K]
700	2.02E+6
800	2.19E+6
900	2.34E+6
1000	2.47E+6
1100	2.58E+6
1200	2.67E+6

Elevation	Inner Fuel 6 - standard 1 - control	Middle Fuel 1 36 - standard 6 - control	Middle Fuel 2 72 - standard 12 - control	Outer Fuel 96 - standard 18 - control	Replaceable Reflectors 66 - hexagonal	Permanent Reflectors 24 - irregular
1.006 m	Top Reflector (709.2)	Top Reflector (4255)	Top Reflector (8511)	Top Reflector (11460)	Top Reflector (66.40)	Top Reflector (25.15)
0.793 m	Fuel Region (559.1)	Fuel Region (3354)	Fuel Region (6709)	Fuel Region (9035)	Side Reflector (52.34)	Side Reflector (19.83)
0.793 m	Fuel Region (559.1)	Fuel Region (3354)	Fuel Region (6709)	Fuel Region (9035)	Side Reflector (52.34)	Side Reflector (19.83)
0.793 m	Fuel Region (559.1)	Fuel Region (3354)	Fuel Region (6709)	Fuel Region (9035)	Side Reflector (52.34)	Side Reflector (19.83)
0.793 m	Fuel Region (559.1)	Fuel Region (3354)	Fuel Region (6709)	Fuel Region (9035)	Side Reflector (52.34)	Side Reflector (19.83)
0.793 m	Fuel Region (559.1)	Fuel Region (3354)	Fuel Region (6709)	Fuel Region (9035)	Side Reflector (52.34)	Side Reflector (19.83)
0.793 m	Fuel Region (559.1)	Fuel Region (3354)	Fuel Region (6709)	Fuel Region (9035)	Side Reflector (52.34)	Side Reflector (19.83)
1.189 m	Bottom Reflector (838.2)	Bottom Reflector (5029)	Bottom Reflector (10060)	Bottom Reflector (13550)	Bottom Reflector (78.47)	Bottom Reflector (29.73)

Figure 2 Diagram of the 48 region FSV RELAP5 model.

The RELAP5 model uses the temperature-dependent thermal conductivity and volumetric heat capacity of un-irradiated H-451 graphite. Table 1 shows thermal conductivities for a bonded fuel compact with a mixture of 11.5% and 50.5% volume packed fissile and fertile particles, respectively [10]. Extrapolation provides values for operating temperatures. Values from the FSV Safety Analysis Report (FSAR) match the extrapolated thermal conductivity. Equation 2 calculates the volumetric heat capacity, with \square in degrees Rankine [1]. Table 2 presents calculated values in terms of J/m³-K.

3. MCNP5-RELAP5 Coupling Using PIKMT Method

Applications of the Ratio and PIKMT methods to the VHTR successfully obtained the nuclear-thermal-hydraulic feedback. The Ratio method is fast, but requires several iterations for the axial temperature distributions to converge. Also, it requires pre-calculated fractions to account for delayed gamma contributions to heat deposition. The PIKMT method requires two MCNP5 runs, more than doubling the MCNP5 run time. However, it takes fewer iterations for the axial temperature distributions to converge [5]. For this project, the PIKMT method accounts for FSV thermal-hydraulic feedback.

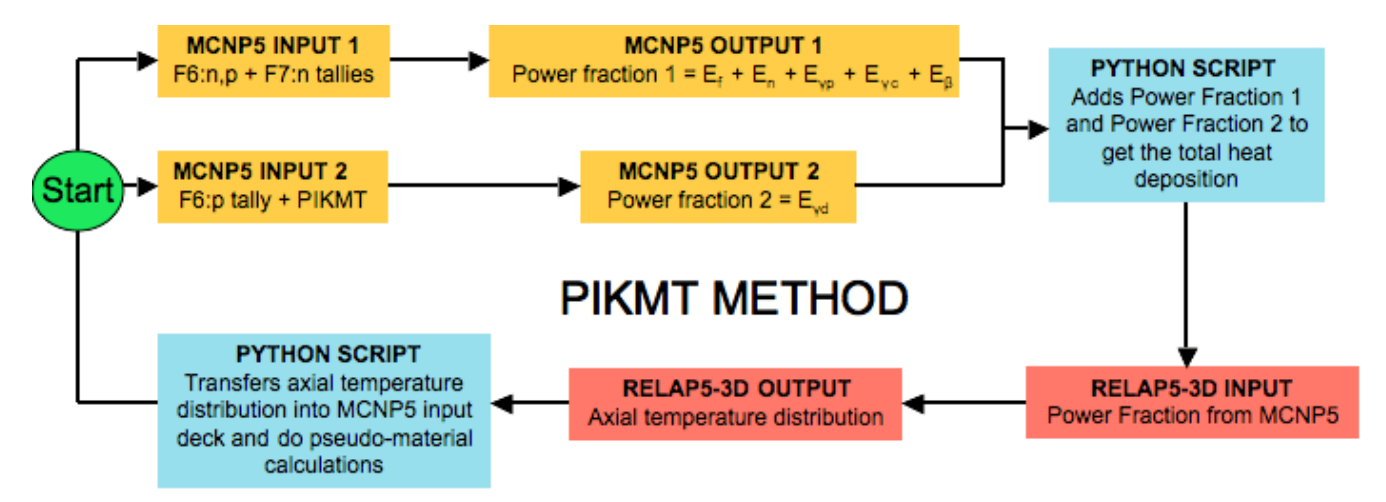


Figure 3 Flow chart of the PIKMT iterative method for calculating power fractions and temperatures.

The PIKMT-required *standard* and *pikmt* runs use F6:n,p + F7:n tallies and a F6:p tally with a *pikmt* card, respectively. The *standard* run provides the energy deposition contributions by neutrons, fission products, beta particles, prompt gammas and capture gammas. The *pikmt* run provides the delayed gamma contribution to energy deposited. Equation 3 calculates the heat deposited using the tallies and 222, 22, and 2, the fission Q-values or fission energy contribution from delayed gammas, prompt gammas, betas, and all particles, respectively.

$$22 = 26.2, 2 + 26.2 22222 + 27.2 222$$
 (3)

A Python script post-processes the MCNP5 outputs, calculating power fractions and making a RELAP5 input deck. RELAP5 uses these fractions to calculate temperature data. Another Python script post-processes the output to produce temperatures for the next MCNP5 power fraction calculation. MCNP5 input decks receive the updated temperatures, and the process repeats until convergence. Figure 3 is a flowchart of the PIKMT method. The RMSD assesses the convergence of the temperatures, calculating the deviation between consecutive iterations.

4. Results

The MCNP5-RELAP5 coupled setup completed nine iterations of the PIKMT method for the initial FSV configuration. Both power fractions and temperatures converge in behaviour similar to that of the VHTR [5]. Figure 4 shows the converged axial temperature distributions in the six radial regions. Material temperature peaks at 1154K in the fourth axial plane of the first middle fuel ring. In the other three fuel rings, temperatures peak in the same axial plane at slightly lower temperatures ranging from 1085K to 1095K. The temperature gradient from the top to core centerline is greater than from the bottom to core centerline. Figure 5 shows the converged axial power distributions in the four fuel regions. The power peaks in the fourth axial plane. The top half of the core generates nearly 65% of the total power.

The top (axial planes 2, 3, and 4) and bottom (axial planes 5, 6, and 7) halves of the FSV active core have different fuel loadings. Depending on the fuel blend, the bottom uranium and thorium loading is 71-76% and 82-90%, respectively, of the top loadings. In the fuel rings, the power in the fifth axial plane is 72-76% of the power in fourth axial plane. This power difference mimics the uranium loading because the uranium drives the fissions in a clean core, and the fission heating is the primary contributor to total heat deposition. The strong Doppler coefficient of reactivity helps depress the power at the high material temperatures in axial planes 6 and 7.

The material temperature depends on the power and the coolant temperature. Coolant temperature increases as it passes down through the reactor. The material temperature is low in the first two axial planes because the coolant is still relatively cold. The material temperature peaks in the fourth axial plane because the power is so high. The rising coolant temperature in axial planes 5, 6, and 7 helps keep the material temperature constant, even though the power continuously decreases.

The reflector regions are the coldest two regions of the core because of the little heat deposited from the lack of fission product heating. Figure 6 shows the power profile in the reflector rings. Figure 7 shows the temperature convergence by plotting the RMSD between temperatures of consecutive iterations. Similarly, figures 8 and 9 show the normalized power convergence of the fuel and reflector regions, respectively. The convergence of the power fractions and temperatures mimic one another. Figures 7 through 9 omit the RMSD's between iterations 1 and 2; it is five times larger than that between iterations 2 and 3.

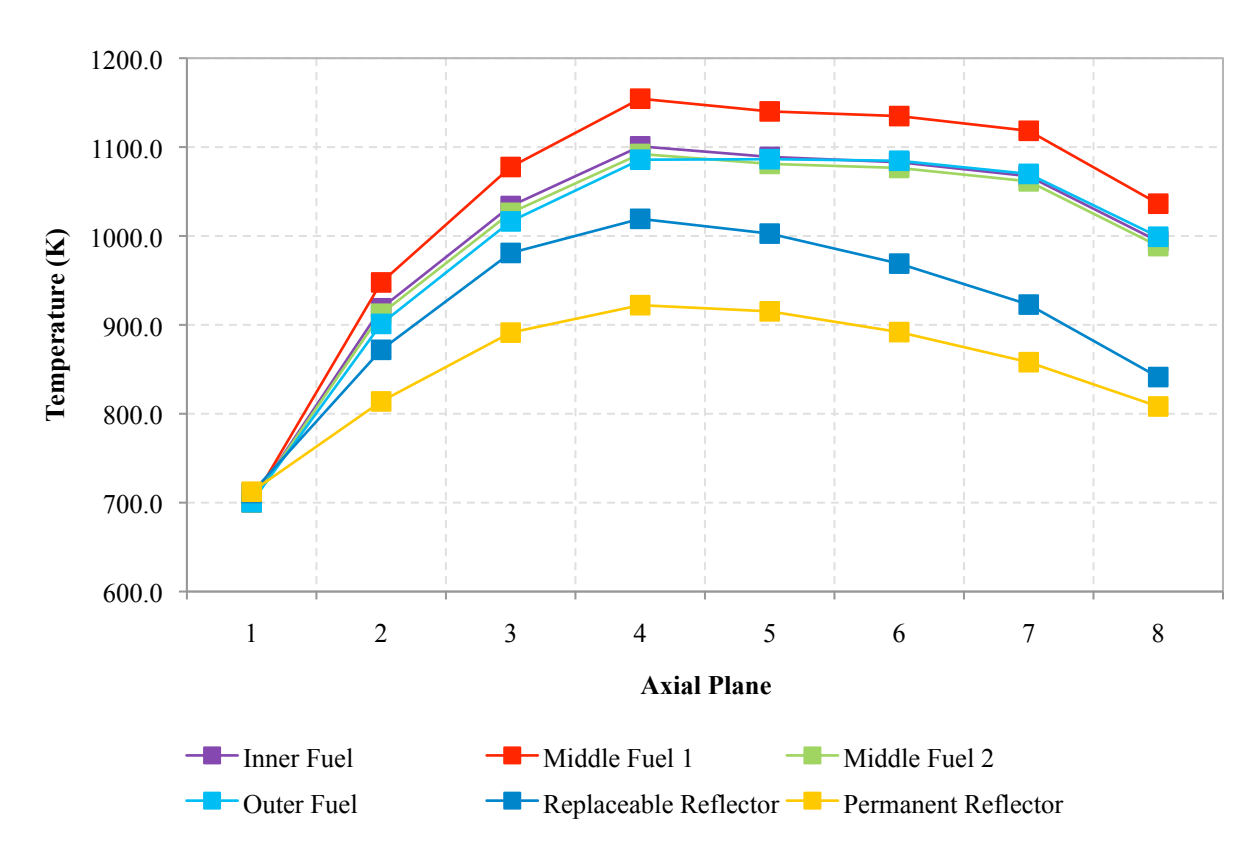


Figure 4 RELAP5 axial material temperature distributions for the six radial rings.

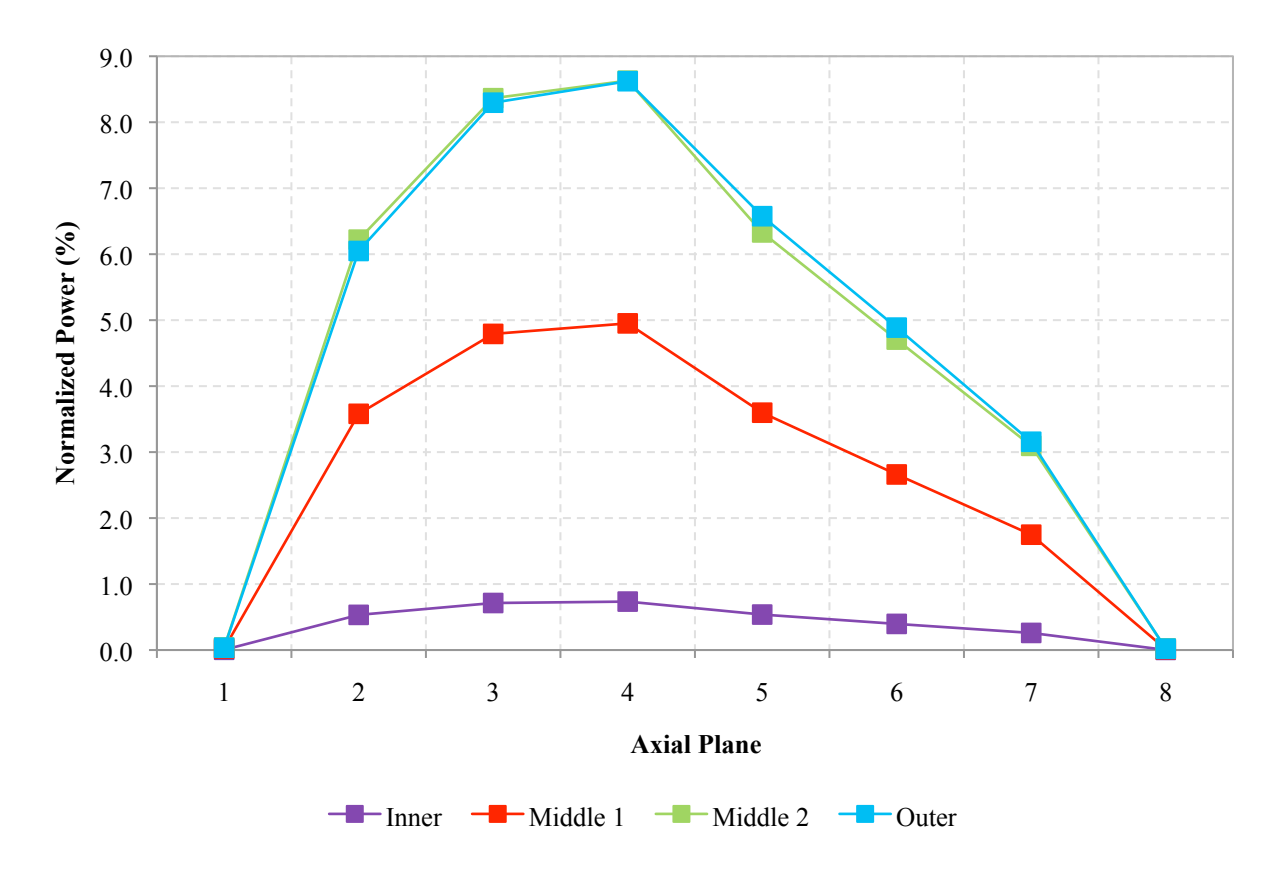


Figure 5 MCNP5 axial normalized power distribution in the fuel rings after 9 iterations.

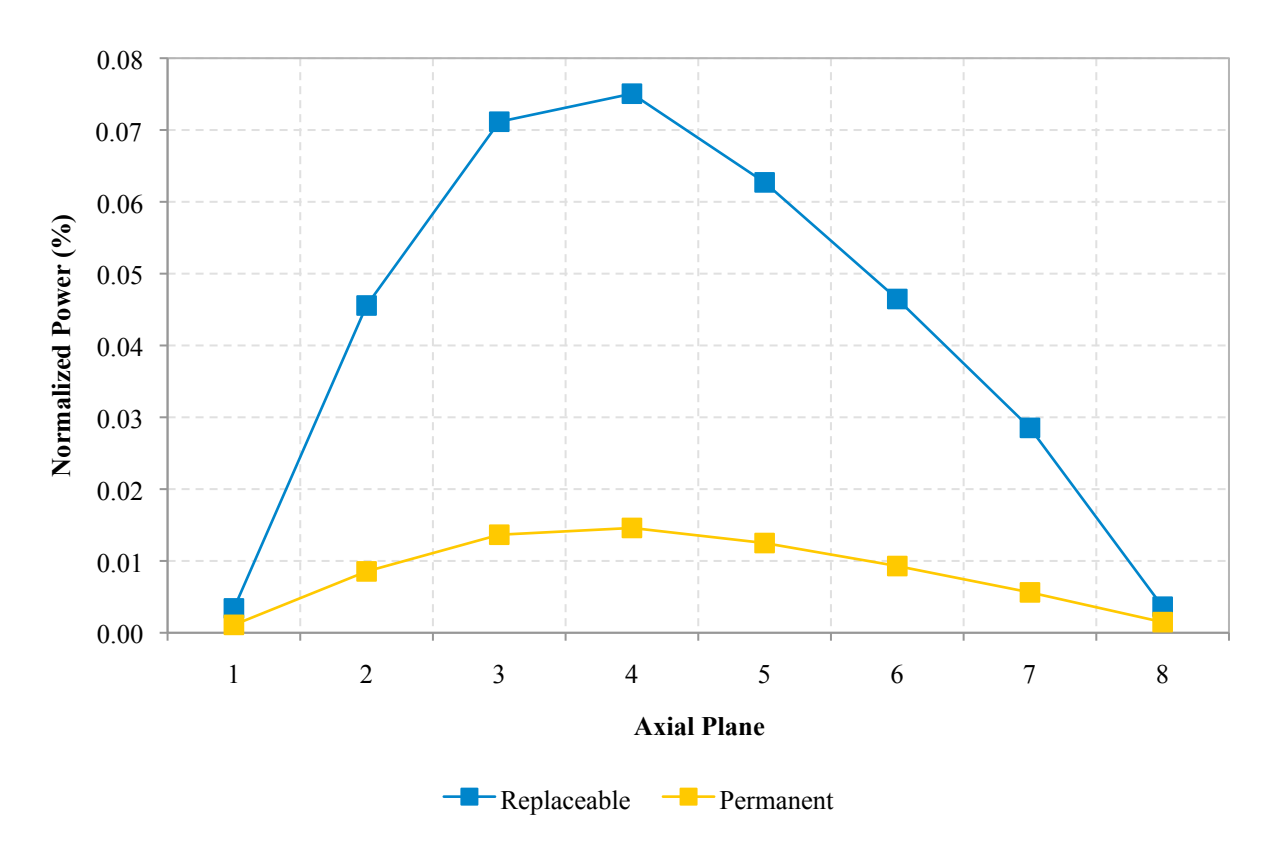


Figure 6 MCNP5 axial normalized power distributions in the reflector rings after 9 iterations.

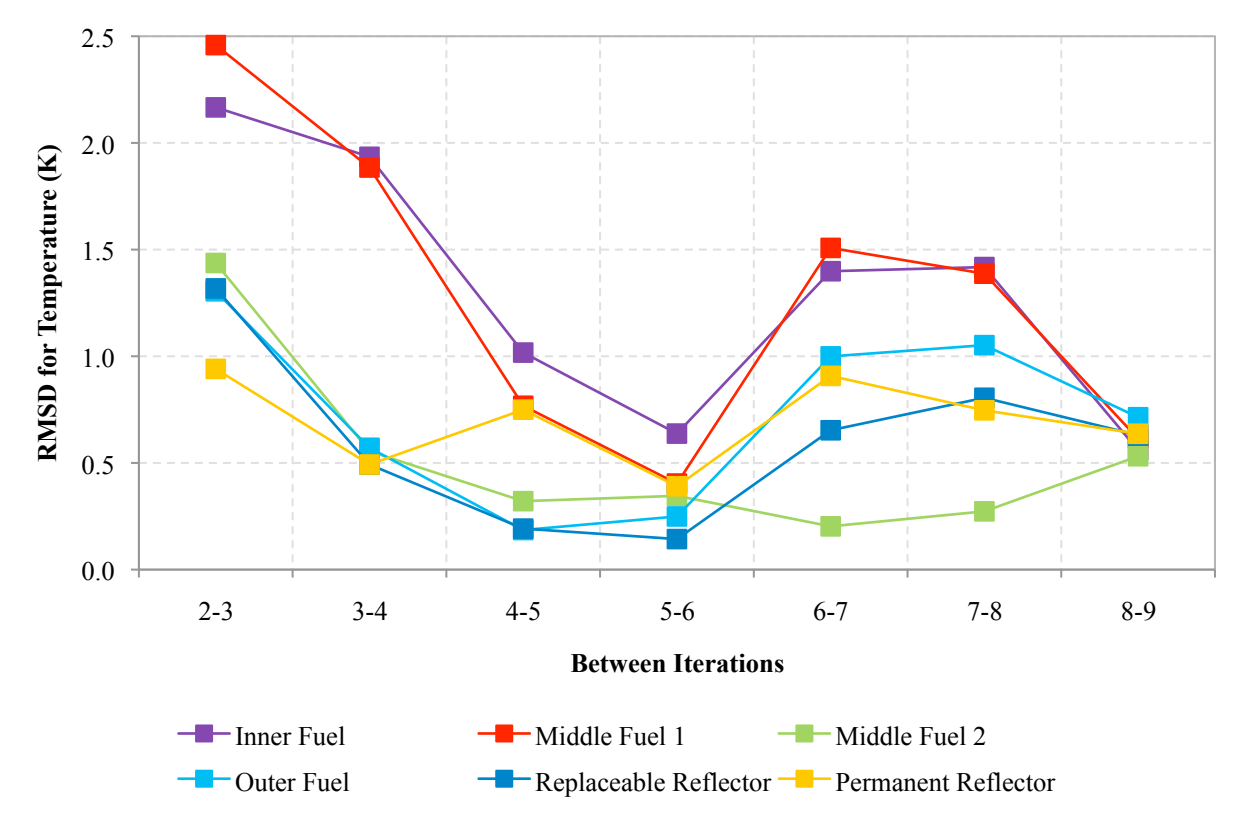


Figure 7 Temperature convergence for the six radial rings.

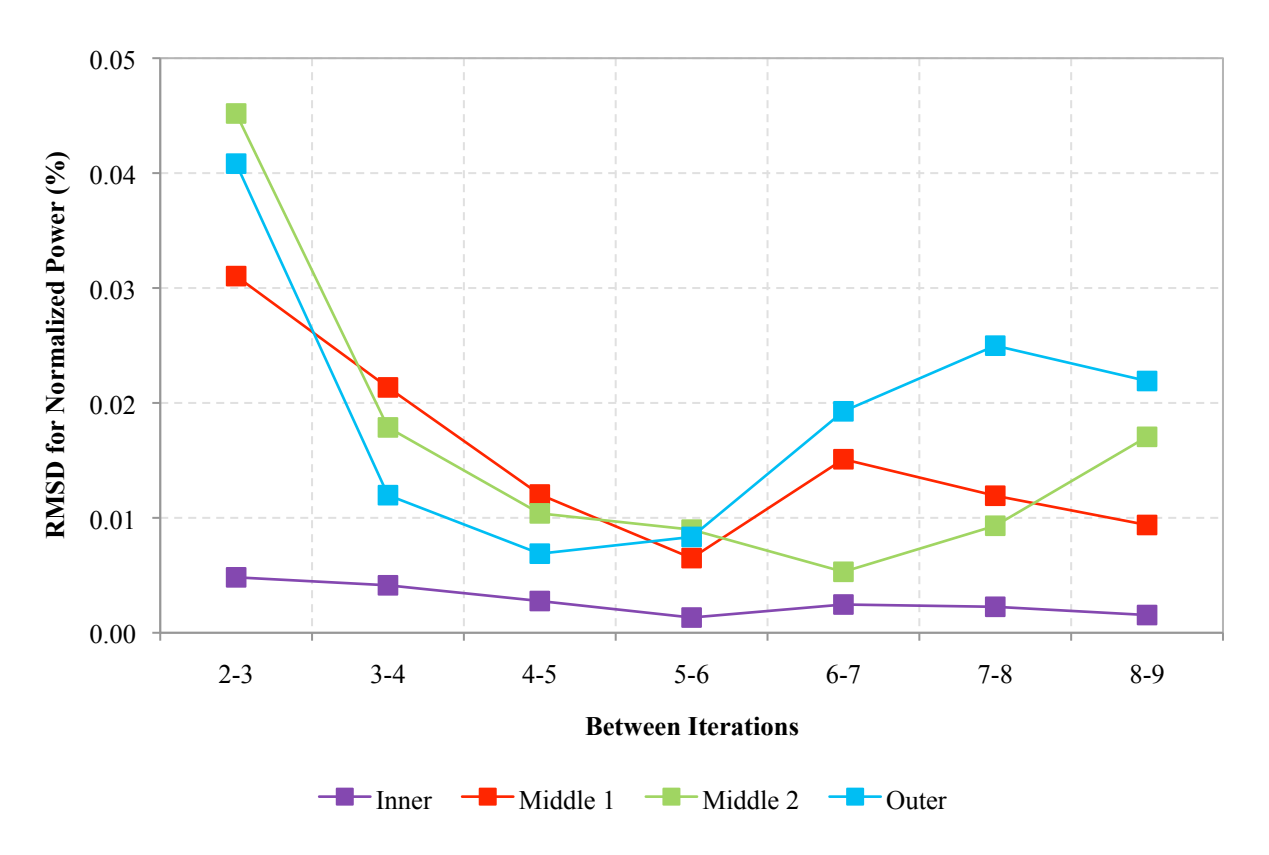


Figure 8 Normalized power convergence in the four fuel rings.

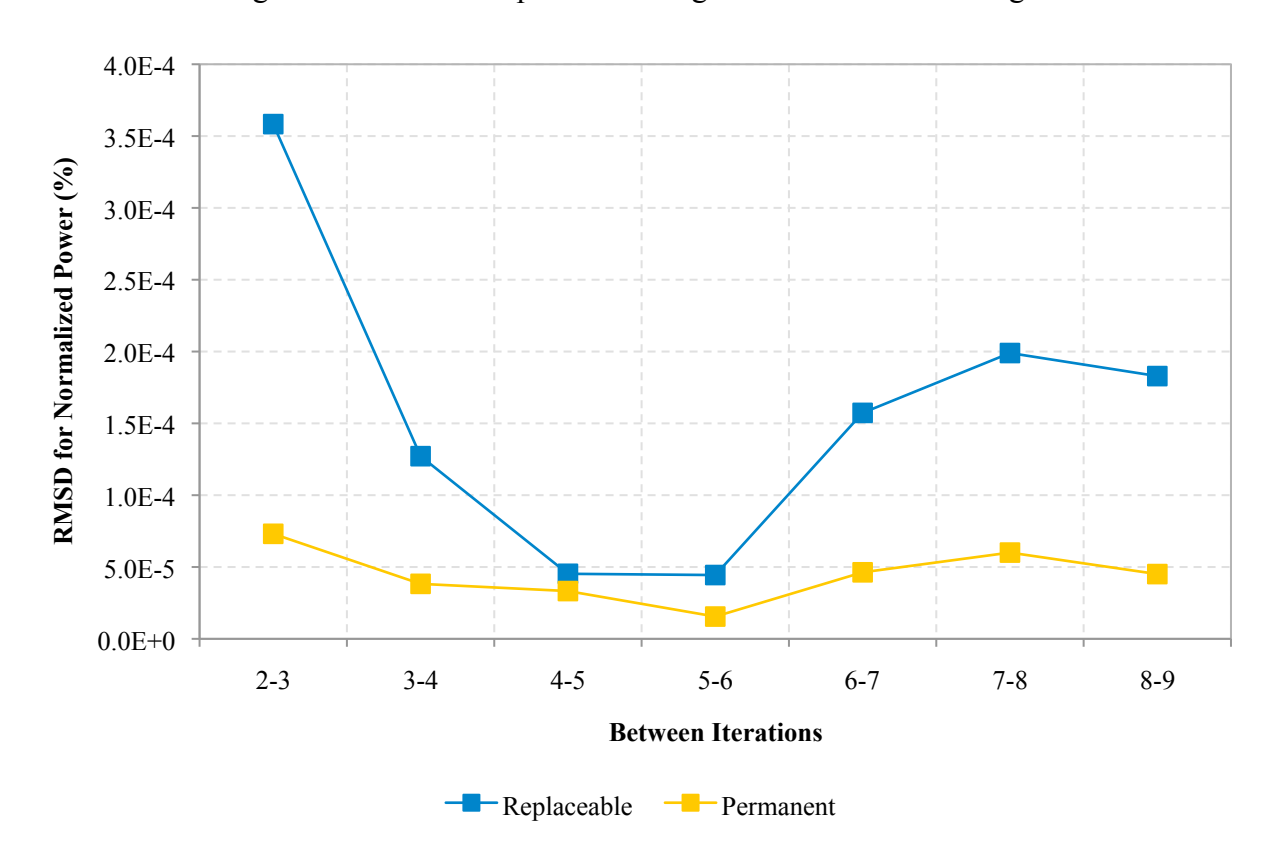


Figure 9 Normalized power convergence in the reflector rings.

4.1 Benchmarking

Due to high temperatures, FSV had no in-core instruments during operation. Region coolant outlet temperatures were the only online measurements. Thus, we are unable to provide a comprehensive temperature benchmark. Temperatures obtained for six axial core zones are insufficient for benchmarking, and are input to the initial MCNP5 power fraction calculation. However, calculated temperatures reflect the inlet and maximum fuel temperature.

GA used a tailored version of GATT [11] known as GATT-2X [12] to calculate power fractions in the fuel regions of FSV for depletion studies. These fractions [9] compare well to those calculated by MCNP5. Tables 3 and 4 show the radial and axial profile comparisons, respectively. A control rod error causes the differences between the two middle rings in table 3. Differences for the top and bottom axial fuel planes in table 4 likely result from a reflector geometry or density error. Generally, GATT is not considered 100% accurate.

4.2 Oscillations After Iteration 5

The RMSD continuously decreases until iteration 6, where the RMSD suddenly increases before settling in subsequent iterations. This phenomenon will be referred to as oscillations. They are small in magnitude: the RMSD for temperature remains below 2 K even after nine iterations, and the RMSD for normalized power remains below 0.03%. Still, understanding the source of these oscillations is useful.

Statistical uncertainties in MCNP5 and Doppler feedback in the fuel are probable sources of these oscillations. The little amount of U-238 in the fissile HEU, 53.0 kg, has a small effect on the Doppler feedback. The large amount of Th-232, 15,900 kg, in both fissile and fertile particles likely drives the Doppler feedback.

Lowering the standard deviations for the MCNP5 tallies dampens the oscillations. To show this, we increase the number of histories per cycle from 250,000 (*short*) to 750,000 (*long*) for the sixth iteration and the PIKMT method runs to nine iterations with this adjustment. This triples the run time but decreases the k-effective standard deviation by a factor of approximately 1.73, and depending on the location and material composition, the standard deviations for tallies decrease by a factor of 1.5 to 2. Figures 10 and 11 compare the temperature oscillations and figures 12 and 13 compare the normalized power oscillations of the *short* and *long* MCNP5 runs. Oscillations for the *long* runs are smaller in comparison to the *short* runs. Table 5 lists the Root-Mean-Square (RMS) values of the oscillations beyond iteration 5. The *short* to *long* ratio shows that the increase in the number of histories per cycle decreases oscillation size by a factor similar to that of the decrease in standard deviation.

Table 3 Calculated radial power distribution.

Fuel Ring	Normalize	%		
ruei King	MCNP5	GATT-2X	Difference	
Inner	3.18	3.16	0.71	
Middle 1	21.4	23.7	9.75	
Middle 2	37.4	35.2	6.27	
Outer	37.6	38.0	0.85	

Table 4 Calculated axial power distribution.

Axial Plane	Normalize	%	
(Fuel only)	MCNP5 GATT-2X		Difference
2	16.4	17.0	3.75
3	22.2	22.4	1.18
4	22.9	22.6	1.70
5	17.0	17.3	1.33
6	12.6	12.9	1.63
7	8.26	7.87	5.02

Table 5 RMS values of the oscillations for the rings in *short* and *long* MCNP5 runs.

Runs	Inner	Middle 1	Middle 2	Outer	Replaceable	Permanent
Short	1.96E-3	1.12E-2	1.10E-2	1.97E-2	1.58E-4	4.48E-5
Long	1.35E-3	4.82E-3	7.41E-3	1.02E-2	8.76E-5	1.96E-5
Short:Long Ratio	1.45	2.32	1.49	1.92	1.80	2.29

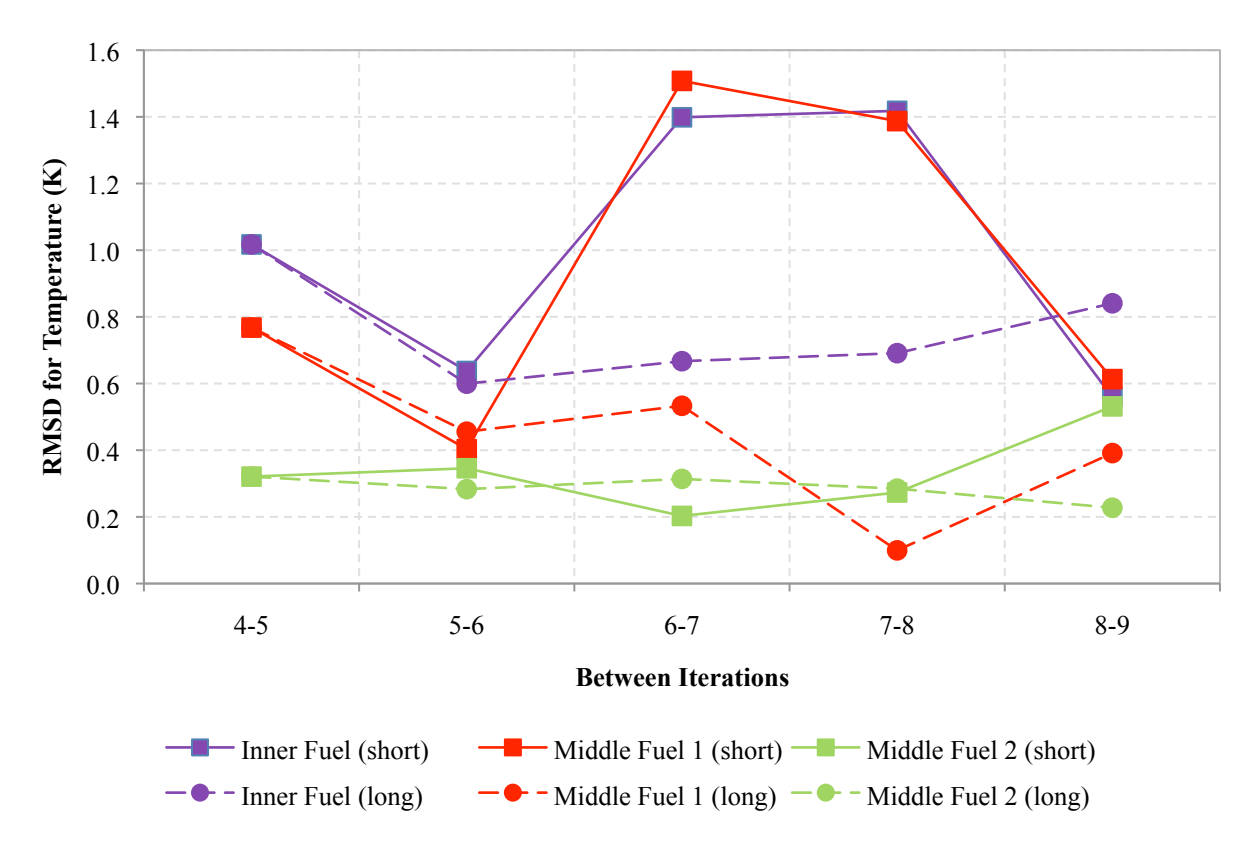


Figure 10 Temperature RMSD oscillations in fuel rings in *short* and *long* MCNP5 runs.

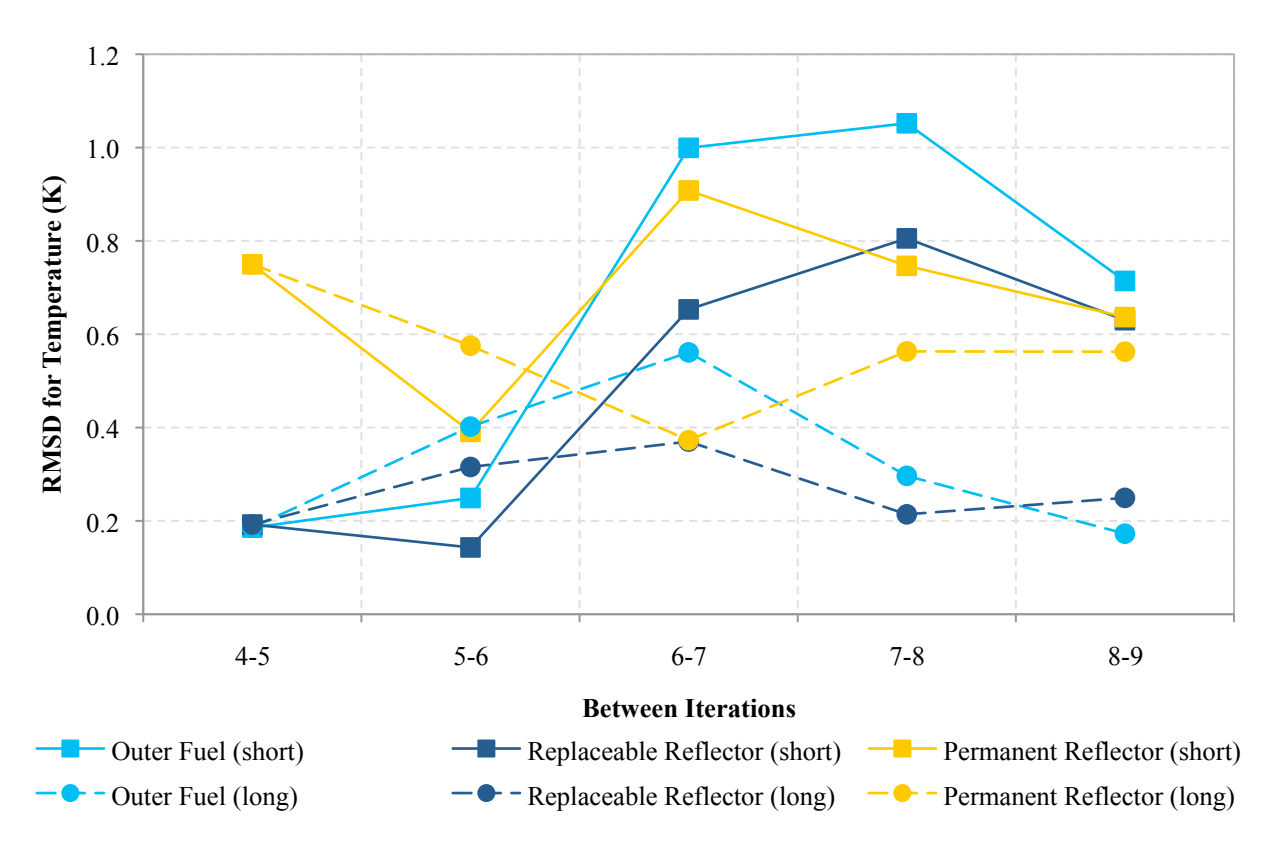


Figure 11 Temperature RMSD oscillations in outer rings after in *short* and *long* MCNP5 runs.

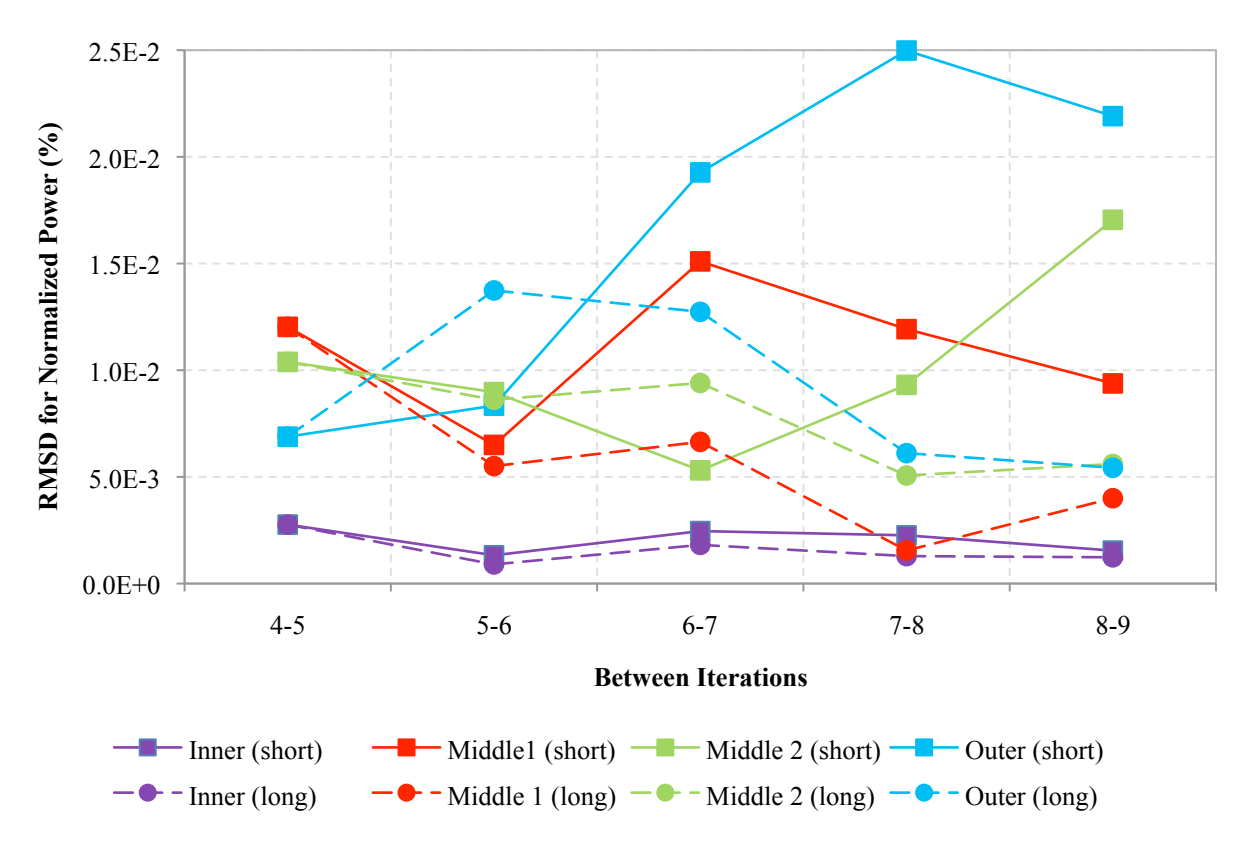


Figure 12 Power RMSD oscillations in the fuel rings after iteration 5 in *short* and *long* MCNP5 runs.

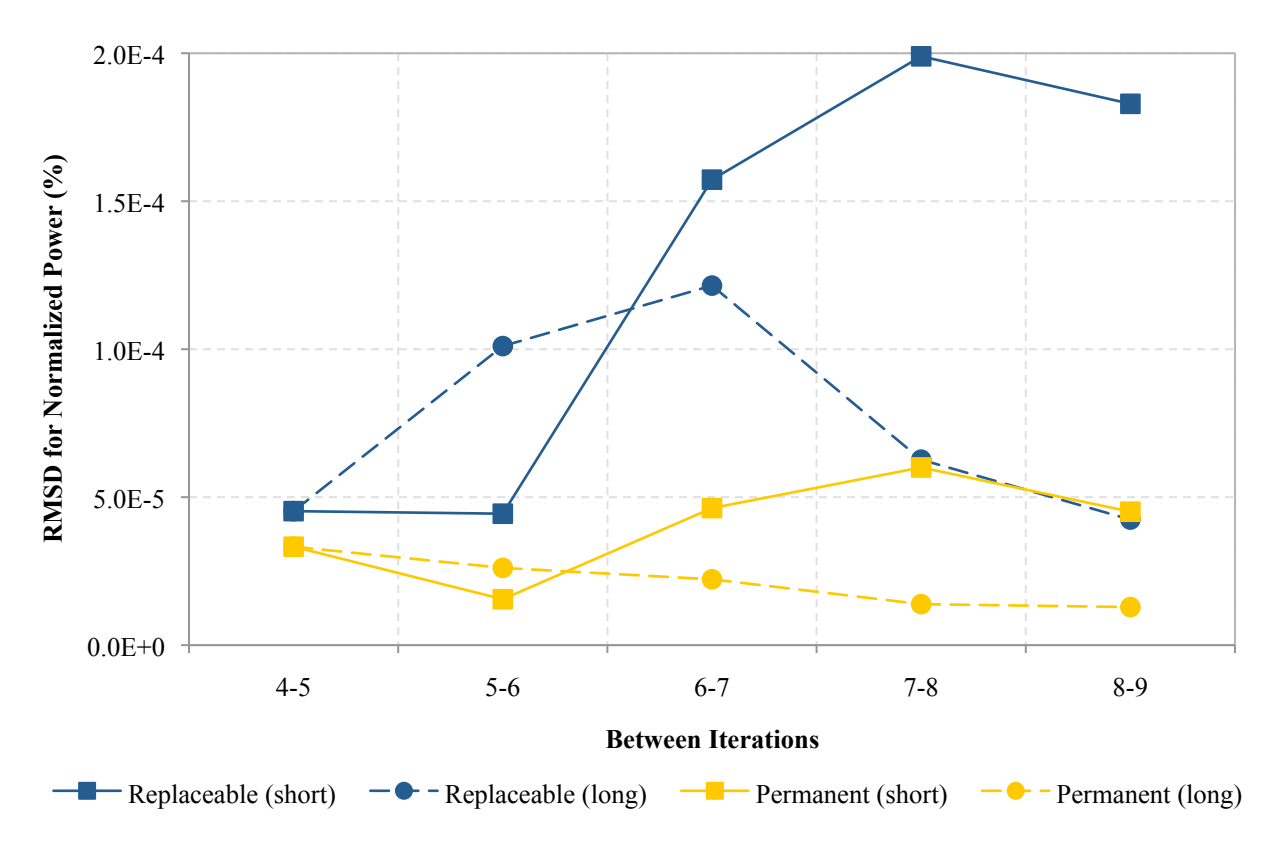


Figure 13 Power RMSD oscillations in reflector rings after iteration 5 in *short* and *long* MCNP5 runs

Table 6 Normalized power RMSD from maximum standard deviation for iteration 8.

Runs	Inner	Middle 1	Middle 2	Outer	Replaceable	Permanent
Short	4.99E-4	1.41E-3	1.89E-3	1.91E-3	3.60E-5	1.85E-5
Long	3.02E-4	9.22E-4	1.08E-3	1.15E-3	2.17E-5	1.05E-5
Short:Long Ratio	1.65	1.53	1.75	1.66	1.66	1.75

Because the heat deposition equation is linear, equation 4 yields the standard deviation of the final calculated value, where the 2-values are standard deviations of their respective tallies. This equation results in a standard deviation for each of the 48 regions. For simplicity, we use the standard deviations as the RMSD to eliminate the axial resolution. Table 6 lists these reduced values, showing that the RMSD's for each ring is one order of magnitude below the RMS values in table 5 and in figures 12 and 13. Thus, MCNP5 statistical fluctuations are not the sole cause of the fluctuation in normalized power between consecutive iterations. But, when MCNP5 receives new temperatures, Doppler feedback has a strong effect on the calculated power distribution. These fluctuating temperatures drive the small oscillations. Regardless, convergence shown in the results section is sufficient for most applications.

5. Conclusion

The MCNP5-RELAP5 coupled calculations yield good results for FSV. MCNP5 calculated power distribution matches GATT calculations. The RMSD for temperatures and normalized power remain below 2 K and 0.03%, respectively, after the ninth iteration of the PIKMT method. MCNP5 uncertainties and Doppler feedback cause small oscillations after iteration 5. Increasing the source particle histories in the MCNP5 dampens oscillations. Tallies from the PIKMT method provide ratios for the Ratio method. This paper represents the best results obtained from available data of FSV.

6. References

- FSAR, "Fort St. Vrain Final Safety Analysis Report," General Atomics Report.
- [1] [2] Monte Carlo Team, "MCNP – A General Monte Carlo N-Particle Transport Code, Version 5," LA-UR-03-1987, Los Alamos National Laboratory (2003).
- The RELAP5-3D Code Development Team, "ATHENA Code Manual," INEEL-EXT-98-[3] 00834, Rev. 2.2, Idaho National Engineering and Environmental Laboratory (2003).
- G. Van Rossum, "Python 2.6.2," Python Software Foundation (2010).
- G. Yesilvurt, K. Banerjee, E. De Villele, J.C. Lee and W.R. Martin, "Coupled Nuclear-Thermal-Hydraulic Calculations for VHTRs," Trans Am. Nucl. Soc. 102, 519 (2010).
- General Atomics Private Data.
- [6] [7] B.R. Betzler, J.C. Lee, and W.R. Martin, "MCNP5 Analysis of Fort St. Vrain High-Temperature Gas-Cooled Reactor", Trans Am. Nucl. Soc. 102, 515 (2010).
- J.L. Conlin, W. Ji, J.C. Lee, and W.R. Martin, "Pseudo Material Construct for Coupled Neutronic-Thermal-Hydraulic Analysis of VHTGR," *Trans. Am. Nucl. Soc.* 92, 225-227, San [8] Diego, CA (June, 2005).
- R.J. Nirschl, "Three Dimensional Depletion Analysis for the 'As-Built' FSV Initial Core," [9] General Atomics Report, GA-A13100, (1975).
- A.S. Shenoy, and D.W. McEachern, "HTGR Core Thermal Design Methods and Analysis," [10] General Atomics Report, GA-A12985, (1974).
- H. Kraetsch, and M.R. Wagner, "GATT: A Three-Dimensional Few-Group Neutron Diffusion [11] Theory Program for a Hexagonal-z Mesh," Gulf General Atomics Report, GA-8547, (1969).
- [12] M. Wagner, and J. Dorsey, "GATT-2X, An External Source Version of the Three Dimensional Diffusion Theory Program, GATT-2," General Atomics unpublished data.